Vol. 5 No. 1 (2005) 45-54

YEMEN ENGINEER
Faculty of Engineering-University of Aden

5 Inclusion of Core Loss Effect in the Simulation of A Cycloconverter FED Induction Motor Drive

Moh'd Zaid A. Karim*

Abstract

Usually, induction motor performance is simulated ignoring magnetic saturation and core loss effects. This leads to inaccurate evaluation. In this paper, these effects are included in the mathematical model of the induction motor. The effect of core loss is incorporated by adding two fictitious windings in the stator along the direct and quadrature axes. The parameters of the 'core loss windings' are obtained experimentally. Further, since the motor, in this work, is fed from a variable frequency supply, the effect of frequency on core loss parameters is considered. Effect of harmonics on core loss resistance is also studied. Using the developed model, the performance of the cycloconverter fed induction motor drive is investigated and presented. Experimental results are also given for comparison.

Key words: magnetic saturation, core loss, cycloconverter, induction motor drive)

ملخص

عادةً يتم إهمال تأثير التشبع المغناطيسي و الفقدان في الحديد عند محاكاة أداء المحركات الحثّية، وهذا قد يجعل تقييم الأداء غير بالغ الدقة.

في هذه الورقة, تم إدخال هذه التأثيرات في التمثيل الرياضي للمحركات الحثّية، حيث يتم إدخال تأثير الفقدان في الحديد بإضافة ملفين تخيليين للجزء الثابت للمحرك باتجاه المحورين المتعامدين. وقد تم الحصول على قيم ملفي الفقدان في الحديد عملياً.

بما إن المحرك المستخدم في هذا البحث قد تم تشغيله من مصدر متغير التردد ، فكان لابد من الأخذ بعين الاعتبار تأثير التردد على قيم ملفي الفقدان في الحديد.

كما تم أيضاً في هذه الورقة دراسة تأثير الموجات التوافقية (التشوهات) الناتجة من محول التردد على مقاومة ملفي الفقدان في الحديد.

باستخدام التمثيل الرياضي للمحرك الحثّي و محول التردد، آخذين بعين الاعتبار التشبع المغناطيسي و الفقدان في الحديد تم القيام بمحاكاة المنظومة أعلاه وعرض النتائج المتحصل عليها وكذلك مقارنتها بالنتائج العملية لتأكيد واثبات صحة المحاكاة.

1. INTRODUCTION

In many applications of induction motors, it is desirable to operate the motor at high flux level, thus allowing the machine to produce higher torque. This can lead to saturation of the main flux path. Main flux path saturation in orthogonal axis models of induction machines has been a subject of a number of research papers [Kovacs, 1982;

*. Electrical Engineering Department, Faculty of Engineering, University of Aden, Yemen

Brown et. al., 1983; Vas et. al., 1984; Kerkman, 1985; Boldea, and Nasar, 1986; Melkebeek,1983; Levi and Vuckovic, 1989 and Lorenz and Novotny, 1990].

In this paper, the generalized equations describing the behavior of the cycloconverter fed squirrel cage induction motor drive is developed taking the effects of core loss and magnetic saturation into account. The system has been analyzed in a synchronously rotating reference frame.
In variable frequency drives, the core loss is no more constant, it varies with frequency. Since the drive under consideration is of such a type, the effect of frequency on core loss is considered by obtaining, experimentally, a relationship between the core loss resistance and the frequency.
The mathematical model of the cycloconverter fed squirrel cage induction motor drive has been used in the present study for the analysis of the drive.

2. MATHEMATRICAL MODEL

The mathematical model of the cycloconverter fed induction motor drive considering the effect of magnetic saturation has been given in [Gupta, et. al., 1995 and A. Karim et. al., 1996]. This mathematical model is modified in the present paper to include the effect of core loss as follows:

2.1 Inclusion of Core Loss Effect

In stator fed machines, the frequency of flux density variation in the rotor core of the induction machine is low under normal operating conditions due to low value of operating slip. Consequently, it causes negligible core loss. Therefore, core losses are considered to take place in the stator only. The effect of core loss can be incorporated by adding two fictitious windings, ‘cds’ and ‘cqs’, in the stator along the direct and quadrature axes as shown in Fig. 1 [Boldea and Nasar, 1987].

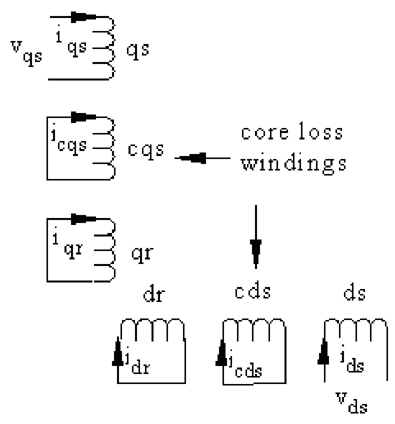

Fig. 1. d-q model including core loss

In Fig. 1, v_{ds}, v_{qs} are the d-q axes stator voltages, i_{ds}, i_{qs} are the d-q axes stator currents, i_{dr}, i_{qr} are the d-q axes rotor currents, i_{cds}, i_{cqs} are the d-q axes core loss currents

From electromagnetic field theory, each winding denoting the core loss has an inductor in series with a resistor [Kraus, 1953 and Plonsey and Collin, 1988]. As the magnetic field diffuses in the core of the machine, it undergoes attenuation and a phase shift. The leakage inductance of the core loss winding is determined by this phase shift. The resistances of these windings depend upon the frequency and the degree of saturation, and their ohmic values can be determined experimentally as given later in this paper.

In present analysis, core loss and saturation will be treated in a unified manner. Therefore, incorporating the effect of core loss, the voltage-current equations of the induction machine can be obtained as follows:

For stator windings

$$v_{ds} = R_s\, i_{ds} + L_{ls}\, pi_{ds} + p\psi_{dm} - \omega_o(L_{ls}\, i_{qs} + \psi_{qm}) \qquad (1)$$

$$v_{qs} = R_s\, i_{qs} + L_{ls}\, pi_{qs} + p\psi_{qm} + \omega_o(L_{ls}\, i_{ds} + \psi_{dm}) \qquad (2)$$

For rotor windings

$$v_{dr} = R_r\, i_{dr} + L_{lr}\, pi_{dr} + p\psi_{dm} - s\omega_o(L_{lr}\, i_{qr} + \psi_{qm}) \qquad (3)$$

$$v_{qr} = R_r\, i_{qr} + L_{lr}\, pi_{qr} + p\psi_{qm} + s\omega_o(L_{lr}\, i_{dr} + \psi_{dm}) \qquad (4)$$

For core loss windings

The voltage-current equations of the core loss windings can be written assuming that the core losses are due solely to the fluxes of the main path.
Therefore from Fig. 1, the d-q axes model will have in addition to Eqns. 1 to 4, two more equations on account of additional core loss windings

$$0 = R_c\, i_{cds} + L_{lc}\, pi_{cds} + p\psi_{dm} - \omega_o\psi_{qm} \qquad (5)$$

$$0 = R_c\, i_{cqs} + L_{lc}\, pi_{cqs} + p\psi_{qm} + \omega_o\psi_{dm} \qquad (6)$$

Where R_s, R_r are stator and rotor resistances respectively; L_{ls}, L_{lr} are stator and rotor leakage inductances respectively; L_m is the magnetizing inductance; R_c and L_{lc} are the resistance and the leakage inductance respectively of the core loss winding; p is the differential operator; ψ_{dm}, ψ_{qm}, are the d-q-axis components of the magnetizing flux, and are given by

$$\psi_{dm} = L_m\, i_{dm}$$

$$\psi_{qm} = L_m\, i_{qm}$$

$$p\psi_{dm} = L_{dm}\, pi_{dm} + L_{dq}\, pi_{qm}$$

$$p\psi_{qm} = L_{qm}\, pi_{qm} + L_{dq}\, pi_{dm}$$

Where L_{dm}, L_{qm} are the d-q axis magnetizing inductances; L_{dq} is the cross saturation inductance; i_{dm}, i_m are the d-q axis components of the magnetizing current.
It should be noted that, since the effect of core loss is included,

$$i_{dm} = i_{ds} + i_{cds} + i_{dr}$$

Similarly

$$i_{qm} = i_{qs} + i_{cqs} + i_{qr}$$

The electromagnetic torque can be obtained as the rotor power contributed by the speed voltage terms divided by the rotor angular speed in mechanical radians per second, thus

$$T_e = (3/2)\,(\mathbf{POLES}/2)\,L_m\,[(i_{qs}+ i_{cqs})\,i_{dr} - (i_{ds}+ i_{cds})\,i_{qr}] \tag{7}$$

Equations (1) to (7) represent the d-q model of the induction motor taking into account the effect of magnetic saturation and core loss [Boldea and Nasar, 1987].
The model of the cycloconverter has been developed by simulating cosine wave crossing principle for determining the triggering instants of the thyristors of the 3-pulse cycloconverter. The voltage waveforms thus obtained at the cycloconverter output consist of a series of segments of the input voltages. These voltages are then transformed into d-q voltages using the transformation equations and are used as the forcing function in the model of the induction motor.

3. IDENTIFICATION OF PARAMETERS OF THE CORE LOSS WINDINGS

The resistance of the core loss windings is obtained, experimentally, by conducting zero slip test. This test has been conducted in the post graduate laboratory of the department of electrical engineering at the University of Roorkee, India. The equivalent circuit of the induction machine under zero slip condition is shown in Fig. 2.

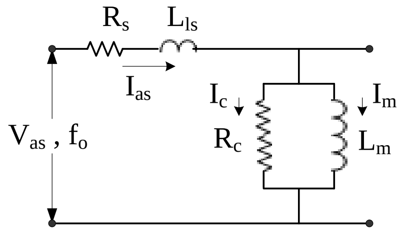

Fig. 2. Equivalent circuit of the induction motor under zero slip condition

The specification and parameters of the motor under consideration is given in the Appendix.
From the above circuit,

$$\overline{V}_{as} - \overline{I}_{as}(R_s + j\omega_o L_{ls}) = \overline{I}_c R_c$$

or

$$R_c = \frac{\left|\overline{V}_{as} - \overline{I}_{as}(R_s + j\omega_o L_{ls})\right|}{I_c} \tag{8}$$

The magnitude of $\overline{V}_{as}$, $\overline{I}_{as}$ and $\overline{I}_c$ are taken as the rms values of input phase voltage and current and core loss current respectively. Squaring Eqn. 8, gives

$$R_c^2 = \frac{\left|\overline{V}_{as} - \overline{I}_{as}(R_s + j\omega_o L_{ls})\right|^2}{I_c^2} \tag{9}$$

The 3-phase input power is

$$P_i = 3I_{as}^2 R_s + 3I_c^2 R_c$$

From which

$$I_c^2 = \frac{P_i - 3I_{as}^2 R_s}{3R_c} \qquad (10)$$

Substituting Eqn. 10 in Eqn. 9 gives

$$R_c = \frac{3\left|\overline{V}_{as} - \overline{I}_{as}\left(R_s + j\omega_o L_{ls}\right)\right|^2}{P_i - 3I_{as}^2 R_s}$$

At nominal frequency (50 Hz), the value of R_c is found to be 5800 Ω. However, for variable frequency drive, the value of R_c varies with the operating frequency (f_o). The variation of R_c with f_o, for present drive is obtained, from the above test, and is given in Fig. 3. The figure reveals approximately, a linear relationship between R_c and f_o. This is in agreement with the relationship given in [Levi et. al., 1996].

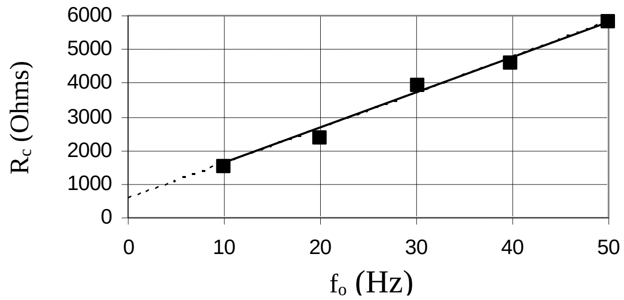

Fig. 3. Variation of R_c with f_o

For comparison, the relationship shown in [Levi et. al., 1996] is presented in Fig. 4. As shown, in the low range frequency, the relation between core loss resistance and the frequency is almost linear. The difference in the numerical values in the two figures is expected because the two machines are different.

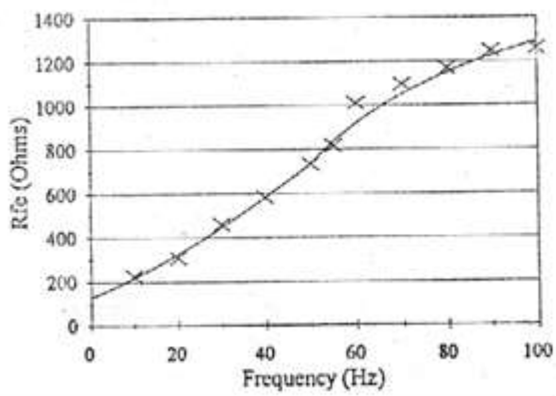

Fig. 4. Variation of core loss resistance and the frequency [Levi et. al., 1996]

It may be noted, in a cycloconverter fed induction motor drive, the operating frequency range is only upto 50/3 Hz only, which ensures linear relationship.
From Fig. 3, the relation between R_c and f_o is obtained as

$$R_c = 105\, f_o + 550 \tag{11}$$

Knowing the values of R_c at any value of f_o, the corresponding value of L_{lc} is obtained as [Boldea and Nasar, 1987]

$$L_{lc} = \frac{R_c}{\omega_o}$$

In cycloconverter fed induction motor drive, the output voltage of the cycloconverter contains a series of harmonic components. Each component contributes to core loss differently. Ideally, to include core loss effect in the simulation of such a drive, each harmonic component is to be considered independently using harmonic equivalent circuit. This clearly would be cumbersome.
If the core loss inductance is assumed to be eliminated from the system equations, then it would be possible to find a weighted stator core loss resistance from harmonic analysis approach, by determining the amplitude and frequency of each harmonic component of the airgap voltage and the corresponding resistance and core loss.
If E_{rms} is the rms value of the total airgap voltage, and P_{ct} be the sum of core losses of all harmonic components, the weighted resistance R_{cw} could be obtained as

$$R_{cw} = \frac{E_{rms}^2}{P_{ct}} \tag{12}$$

This is found to be higher than R_{c1}, the value calculated considering the fundamental component of airgap voltage E_1 and the corresponding core loss P_{c1}. It has been found that using this weighted resistance in the simulation of the present drive, the amount of core loss is essentially the same as the sum of the core losses caused by each harmonic component considered separately.

Under sinusoidal supply, the equivalent core loss inductance has no effect during steady state and can be omitted. But in case of cycloconverter supply, however, the effect of core loss inductance does not completely vanish, due to the fact that the rate of change of d-q core loss currents is not zero. In such a case, using the weighted resistance as in Eqn. (12) in the model, the amount of the calculated overall core loss is found to be smaller than that obtained by considering the harmonic components separately. Since the performance of the drive is dominated by the fundamental component, this situation may be corrected by calculating the weighted resistance based on the fundamental component of the airgap voltage E_1 and the overall core loss P_{ct} as

$$R'_{cw} = \frac{E_1^2}{P_{ct}} \tag{13}$$

This is smaller than R_{c1}. Using this method of weighting in the drives model, the calculated core loss is found to be more close to that obtained from harmonic analysis approach. It has also been observed that the weighted resistance obtained by Eqn. (13), does not differ much from the steady stat value under sinusoidal supply. The difference between the two resistances is found to be 3 %. Therefore, using the steady state core loss resistance based upon sinusoidal supply, as an equivalent resistance in the drives model, could be a reasonable approximation. This approximation is used in this paper.

4. DRIVES PERFORMANCE

The developed mathematical model of the cycloconverter fed induction motor drive is simulated to investigate the drives performance considering the effect of magnetic saturation and core loss. The simulation has been carried out over the complete low frequency range of the cycloconverter under full load condition. For presentation, typical results are given in Figs. 5 to 7, at 10 Hz. At this operating frequency, the value of core loss resistance is found, from Eqn. (11), to be 1600 Ω. The corresponding experimental results are also shown in these figures for comparison. The comparison reveals that the developed mathematical model is satisfactorily simulating the performance of the drive. A close examination of the results reveals a great agreement between the simulated and the experimental ones. The effect of core loss on the induction motor performance has also been studied in the entire range of cycloconverter frequency under full load condition. It is found that, by including core loss in the model of the induction motor, the steady state electrical waveforms and the developed torque are almost unaffected, but the output power and speed get reduced.

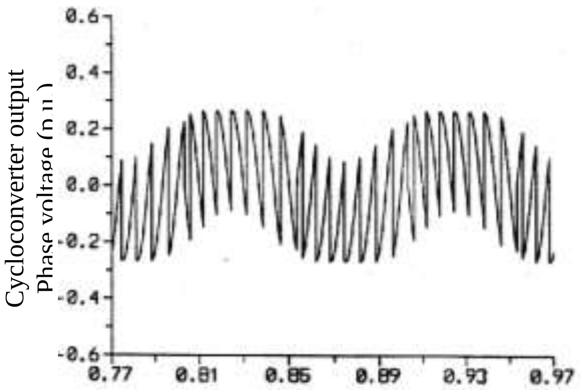

Time (sec)

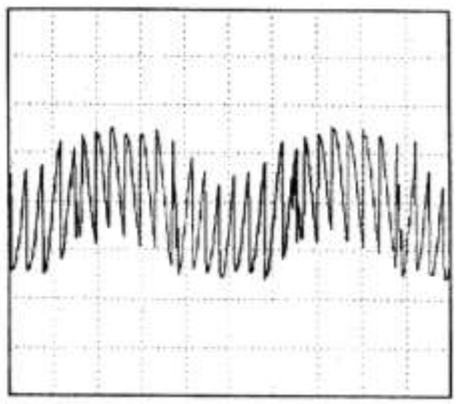

Time scale = 20 ms/div.
Voltage scale = 0.17 p.u./div

(a) simulated waveform (b) experimental waveform

Fig. 5. Cycloconverter output phase voltage (f_o = 10 Hz, full-load)

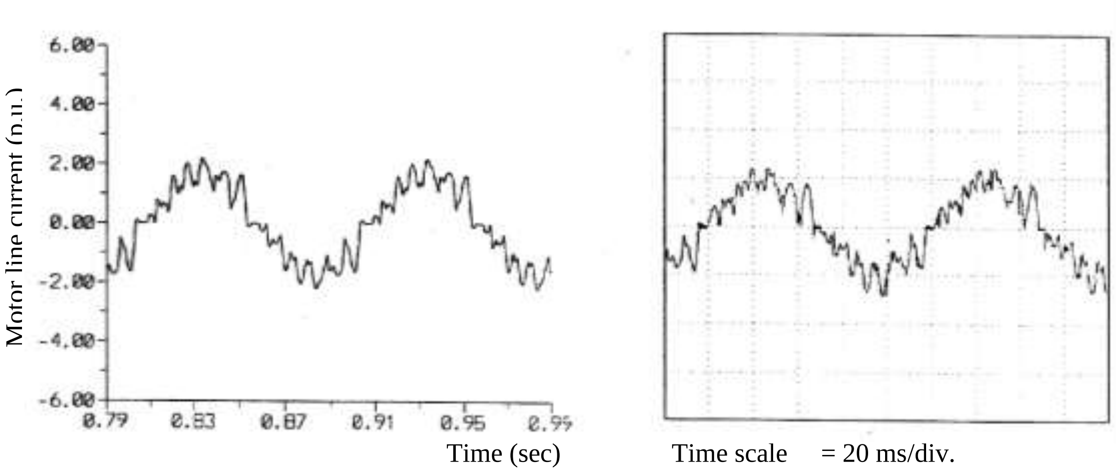

Time scale = 20 ms/div.
Current scale = 1.65 p.u./div

(a) simulated waveform (b) experimental waveform

Fig. 6. Motor line current (f_o = 10 Hz, full-load)

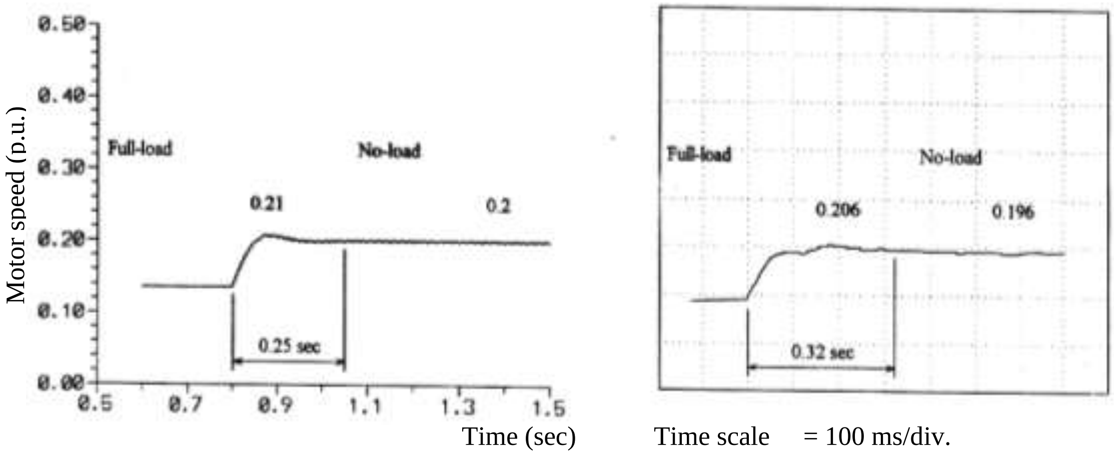

Time scale = 100 ms/div.
Speed scale = 0.067 p.u./div

(a) simulated result (b) experimental result

Fig. 7. Motor speed during step change in load torque at 10 Hz
(full-load to no-load)

5. CONCLUSION

A mathematical model of the cycloconverter fed induction motor drive which considers saturation and core loss effects is presented. The value of core loss resistance is properly selected according to the operating frequency. This is done by experimentally conducting zero slip tests at different operating frequencies. Effect of harmonics on core loss resistance is also studied. Typical simulated performance characteristics are presented. The agreement between the simulated and the experimental results reveals the effectiveness of the developed mathematical model.

References

A. Karim, Moh'd. Zaid, S. P. Gupta and M. P. Dave, 1996. Analytical investigation on a full wave cycloconverter fed induction motor drive including effects of magnetic saturation, ICEMA'96, Harbin, CHINA, pp. 76-79.

Boldea, I., S.A. Nasar, 1987. Unified treatment of core losses and saturation in the orthogonal-axis models of electrical Machines, IEE proc., Vol. 134, Pt. B, No. 6, pp. 355-363.

Boldea, I., S.A. Nasar, 1986. Upon unitary treatment of magnetic saturation in orthogonal axis models of electric machinery, Proc. of the ICEM-86, Munich, pp. 172-175.

Brown, J.E., K.P. Kovacs and P.Vas, 1983. A method of including the effects of main flux path saturation in the generalized equations of A.C. machines, IEEE Trans. on Power App. and Systems, Vol. PAS-102, No. 1, pp. 96-103.

Gupta, S.P., R.A. Gupta, and Bhim Singh, 1995. An improved analysis of a cycloconverter fed cage induction motor drive, Proc. of the International Conf. on Electrical Machines, CICEM'95, Hangzhou, China.

Kerkman, R.J., 1985. Steady-state and transient analyses of an inductionmachine with saturation of the magnetizing branch, IEEE Trans. on Ind. Appln., Vol. IA-21, No. 1, pp. 226-234.

Kovacs, K.P. 1982. Transient performance of an induction machine with variable saturation, Proc. of the ICEM-82, Budapest, pp. 84-86.

Kraus, J.D., 1953. Electromagnetics, (Book), McGraw-Hill Book company Inc.

Vas, P., J.E. Brown, K.E. Hallenius, 1984. Cross-saturation effects in saturated smooth-air-gap machines, Proc. Of ICEM-84, Lausanne, Switzerland, pp. 261-264.

Levi, E., M. Sokola,A. Boglietti and M. Pastorelli, 1996. Iron loss in rotor flux oriented induction machines: identification, assessment of detuning and compensation, IEEE Trans. on Power Electronics., Vol. 11, No. 5, pp. 698-709.

Levi, E. and V. Vuckovic, 1989. Field-oriented control of induction machine in the presence of magnetic saturation, Electrical Machines and Power Systems, Vol. 16, pp. 133-147.

Lorenz, R.D. and D.W. Novotny, 1990. Saturation effects in field-oriented induction machines, IEEE Trans. on Industry Application, Vol. 26, No. 2, pp. 283-289.

Melkebeek, J.A.A.,1983. Magnetising field saturation and dynamic behaviour of induction machines, part-1: Improved calculation method for induction machine dynamics", IEE Proc., Vol. 130, Part B, No. 1, pp. 1-9.

Plonsey, R., R.E. Collin, 1988. Principle and application of electromagnetic fields, Tata McGraw-Hill.

Appendix

Machine's specification

3-phase, 2.2 kW, 4-poles, 415 V , 50 Hz, 4.9 A, delta connected cage induction motor.

Machine's parameters (per unit)

R_s = 0.06, R_r = 0.07, X_{ls} = 0.11, X_{lr} = 0.11, X_m (unsat.) = 2.67, H = 0.21 sec.

Base values

V_b = 586.9 V, I_b = 4.0 A, Z_b = 146.7 Ω, P_b = 3521 W, T_b = 22.4 N.m, N_b = 1500 rpm